Tectonophysics, 178 (1990) 89–107
Elsevier Science Publishers B.V., Amsterdam – Printed in The Netherlands

A mildly depleted upper mantle beneath southeast Norway: evidence from basalts in the Permo-Carboniferous Oslo Rift

E.-R. NEUMANN [1], B. SUNDVOLL [1] and P.E. ØVERLI [2]

[1] *Mineralogisk-Geologisk Museum, Sarsgt. 1, 0562 Oslo 5 (Norway)*
[2] *Amoco Norway Oil, P.O. Box 388, 4001 Stavanger (Norway)*

(Received September 25, 1989; revised version accepted November 10, 1989)

Abstract

Neumann, E.-R., Sundvoll, B. and Øverli, P.E., 1990. A mildly depleted upper mantle beneath southeast Norway: evidence from basalts in the Permo-Carboniferous Oslo Rift. In: E.-R. Neumann (Editor), Rift Zones in the Continental Crust of Europe—Geophysical, Geological and Geochemical Evidence: Oslo–Horn Graben. *Tectonophysics*, 178: 89–107.

Major and trace element compositions and Rb–Sr and Sm–Nd relations are presented for a series of 290–300 Ma old basaltic lavas (B_1) from Vestfold and for the single B_1 flow at Krokskogen in the Permo-Carboniferous Oslo Rift. The Vestfold sequence consists of subalkaline to alkaline basalts, potassic trachybasalts and shoshonites. At Krokskogen B_1 is a subalkaline basalt. The Vestfold basaltic lavas show a relatively wide range in trace element concentrations, and Ta-enriched trace element abundance patterns. Ratios between pairs of incompatible elements show small, but significant variations, e.g., Th/Ta: 1.2–1.8. The highest Th/Ta (2.1) is found in the Krokskogen basalt. A Th/Ta of 1.2 is typical of MORB and OIB, whereas the ratio 1.8 is typical of the lower crust. This variation in Th/Ta is not linked to trace element concentrations, but is accompanied by a regular shift in age-corrected ε_{Nd}, ε_{Sr} and $^{206}Pb/^{204}Pb$ from +4.1, −10 and +19.2 to −1, +18 and +17.7, respectively.

The observed variations in incompatible element ratios, initial isotopic ratios and trace element concentrations are interpreted as follows: The basaltic magmas which gave rise to the Vestfold and Krokskogen lavas originated in lithospheric mantle, which was mildly depleted with respect to Nd–Sr isotopic ratios but relatively rich in radiogenic Pb (PREMA-type). These magmas were retained in the lower crust where they crystallized ol + cpx; some of the magmas were also contaminated. The highest degree of contamination is seen in the lower part of the Vestfold sequence and in the Krokskogen basalt. At the present level of information about the Oslo Rift (no data are available for its southern, submerged part), rift magmatism appears to be dominated by a PREMA source in the pre-rift lower lithosphere. The dominance of a lithospheric mantle source in the rift magmatism suggests that the Oslo rifting event was initiated by passive mechanisms.

Introduction

In recent years, considerable efforts have been made to increase our understanding of the nature, dynamics and evolution of the continental lithosphere. Many important questions concern intracontinental magmatic activity: (a) how and where are magmas generated; (b) what, if anything, do they tell us about the geochemical character of the lower continental lithosphere; and (c) which chemical and mineralogical transformations are induced in the mantle and crust by intraplate magmatic activity? Continental rifts represent one tectonic setting where magmatic products may be used to increase our understanding of the continental lithosphere.

Investigations concerning the impact of a rifting event on different parts of the lithosphere are

0040-1951/90/$03.50

being pursued in the Permo-Carboniferous Oslo Rift in southeastern Norway. During the last decade extensive data have been presented on the compositional relations of various rock types and their minerals. The data have been used to model the origin and evolutionary history of various rock types.

In this paper we present major, trace element and Nd–Sr isotopic data on two important groups of basaltic lavas in the Oslo Rift, that is B_1 in Vestfold and in Krokskogen. This information is used to test previous models for the isotopic characteristics and location of mantle sources involved in the generation of the Oslo Rift magmas. The implications of source location for rift mechanism are discussed. We also use information from this and earlier studies on the Oslo Rift to deduce changes imposed by rift-related magmatic processes on different parts of the crust.

Geological setting

The Precambrian basement east and west of the Oslo Rift consists of metasedimentary rocks, granitic gneisses, metagabbros, granites and migmatites which underwent an amphibolite-grade metamorphism with partial melting 1000–1200 Ma ago. Remnants of an older granulite facies metamorphism have been observed southwest of the Oslo Region (e.g., Jacobsen and Heier, 1978; Field and Råheim, 1979; Hageskov and Pedersen, 1981; Skjernaa and Pedersen, 1982; Dahlgren, 1987). Within the rift area, the Precambrian basement is overlain by folded Cambro-Silurian shales and limestones. These rocks are unconformably overlain by a Late Carboniferous series of sedimentary rocks (the Asker Group) representing subaerial alluvial sedimentation and a shallow marine transgression. The Asker Group is conformably overlain by Oslo Rift basalts (e.g., Henningsmoen, 1978; Olaussen, 1981).

Magmatism in the Oslo Rift occurred from about 300 to 240 Ma ago. The extensional period started with formation of grabens and simultaneous extrusion of large volumes of basaltic lavas, the B_1 series. The B_1 basalts are almost entirely covered by younger lavas (see below), but are exposed in the Skien area, along the eastern margin

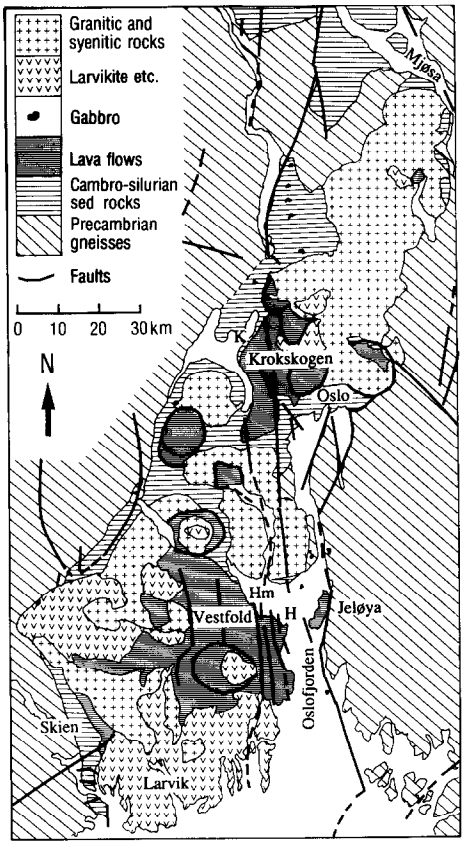

Fig. 1. Simplified geological map of the Oslo Rift, based on maps by Oftedahl (1960), Larsen (1975), Ramberg and Larsen (1978) and K.Y. Buer (pers. commun., 1989). Sample localities are indicated by *H* (Horten), *Hm* (Holmestrand) and *K* (Krokskogen).

of the Vestfold lava field, at Jeløya, and along the western and southern margin of the Krokskogen lava field (Fig. 1). The B_1 lavas show a northwards decrease in thickness and alkalinity. The $\leqslant 1500$ m thick lava sequence in the Skien area in the southern part of the Oslo Region consists of nephelinites and basanites (TAS classification of Le Bas et al., 1986) in the lower part, and alkaline basalts in the upper part. *Mg*-numbers ($Mg/(Mg + Fe_t)$) are 0.54–0.67. Thickness and alkalinity decreases northwards. In the Vestfold–Jeløya area, the B_1 sequence is subalkaline to mildly alkaline and shows large local variations in thickness (180–1500 m). West and north of Oslo, B_1 consists of a single 15–30 m thick flow of aphyric subalkaline basalt; further north it is absent (Oftedahl, 1952; Weigand, 1975; Ramberg and Larsen, 1978;

Sundvoll, 1978; Segalstad, 1979; Sundvoll and Larsen, 1982; Øverli, 1985; Tollefsrud, 1987; Schou-Jensen and Neumann, 1988).

The B_1 volcanism was succeeded by the extrusion of numerous flows of rhomb-porphyry (RP) lavas (trachyandesitic composition), although some basalt flows occur within the RP sequence. Trachytic lavas and ignimbrites are common towards the top of the lava sequence. The presence of large rhomb porphyry dykes within the graben and on its flanks ($\leqslant 40$ m wide) suggests that fissures represented important pathways for magma ascent through the upper crust. The extrusive period culminated with the formation of central volcanoes, many of which developed into calderas (e.g., Brøgger, 1933; Oftedahl, 1953; Ramberg and Larsen, 1978; Larsen and Sundvoll, 1983).

A series of small intrusions of layered gabbro (formerly called "Oslo-essexite") (266 ± 6 Ma) may represent feeders to basaltic central volcanoes (Neumann et al. 1985).

During and after the time of cauldron formation a number of large, nearly circular, felsic batholiths were emplaced into the shallow crust (Fig. 1). These composite plutons are trachyandesitic (e.g., larvikites) to granitic in composition, and, like the felsic lavas, they became increasingly silicic with time. It has been proposed that the period of extensional stress ended before (or during) the stage of caldera formation and batholith emplacement (e.g., Sæther, 1962; Sundvoll and Larsen, 1982; Larsen and Sundvoll, 1983; Ramberg and Morgan, 1984; Rasmussen et al., 1988).

The igneous activity in the Oslo Rift was accompanied by considerable dyke emplacement. The major dykes are contemporaneous with the main phase of magmatic activity. K–Ar ages down to 190 ± 6 Ma suggest however that dyke emplacement continued for a considerable time after the rifting event, but these ages have, so far, not been confirmed by other methods (Neumann, 1960; Dons, 1977; Sundvoll et al., 1990).

It is estimated that uplift and erosion have removed the uppermost 1–3 km of the Permian upper crust (Oftedahl, 1952), exposing the roots of the Oslo magmatic complex.

Petrography

B_1 basaltic lavas, Vestfold

The B_1 basaltic lava sequence in Vestfold (Fig. 1) was sampled at two localities: one near the town of Horten, where each of 39 lavas has been sampled from a 170 m thick exposure (Øverli, 1985); the other near the town of Holmestrand, where 7 successive lavas have been sampled from a 90 m thick exposure. Both the upper and the lower parts of the Holmestrand sequence is covered by Quaternary sediments. The lavas are listed according to stratigraphic position in Table 1.

The lavas have been divided into 4 groups on the basis of their phenocryst content: cpx–ol (CO), plag–cpx–ol (PCO), plag (P) and aphyric lavas. The Horten profile shows systematic upsection petrographic variations (see Table 1); the lower part consists of CO and aphyric basalts; the upper parts of PCO and P lavas, with aphyric lavas rare. The Holmestrand profile consists of alternating CO and PCO basalts. The Horten lavas have been described in detail by Øverli (1985), from which a summary of the petrography is given below.

In *CO basalt*, augite is the dominant phenocryst phase. It occurs as zoned, euhedral crystals up to 5 mm long, or of clusters of crystals. Pseudomorphs of serpentine, chlorite, calcite and oxides after olivine are present as single grains ($\leqslant 3$ mm in diameter), inclusions in the cores of augite phenocrysts or aggregates. Up to 2 mm long, euhedral to subhedral phenocrysts of $magnetite_{ss}$ occur as isolated grains, or as inclusions in the rims of augite phenocrysts. Phenocrysts make up 15–40% of the rock volume. The groundmass is fine-grained to aphanitic and somewhat altered, and in some pyroxene basalts it appears to represent devitrified glass. Augite, pseudomorphs after olivine, $magnetite_{ss}$ + ilmenite, apatite and feldpar have been identified in the groundmass. The groundmass is partly altered to clinozoisite, sericite, biotite, chlorite, calcite and Fe–Ti-oxides. Miarolitic cavities filled by calcite, chlorite, laumontite + quartz make up 2–3% of the rocks.

The *PCO basaltic lavas* resemble the CO basalts, but carry phenocrysts of plagioclase ($\leqslant 10$

mm long) in addition to pseumorphs of olivine ($\leqslant 5$ mm), zoned augite ($\leqslant 15$ mm) and magnetite ($\leqslant 1$ mm). Like magnetite$_{ss}$, plagioclase phenocrysts occur in some cases as inclusions in the rims of augite. Phenocrysts generally make up 10–30% of the rock volume, but reach 50% in FX0. The groundmass is dominated by plagioclase, augite, magnetite and ilmenite. Secondary minerals and miarolitic cavitites as in CO basalts, the degree of alteration varies.

TABLE 1

Representative major and trace element analyses of B_1 basaltic rocks from Vestfold and Krokskogen. The samples from Vestfold are listed according to stratigraphic position in two profiles, FA1 at the base, FZ at the top of the Horten profile; OB102 at the base, OB96 at the top of the Holmestrand profile

	Vestfold, Horten profile									
	CO FA1	CO FA2	CO FA3	CO FA4	CO F1	CO F2	CO F3	CO F4	CO F6	CO F8a
Major elements (wt.%)										
SiO_2	44.27	48.68	44.34	52.45	42.78	42.97	43.43	43.18	41.20	48.15
TiO_2	5.42	5.12	5.43	4.90	5.08	5.12	5.09	5.03	5.14	4.34
Al_2O_3	9.61	9.94	11.20	10.42	7.89	7.85	8.18	8.07	7.33	10.16
$Fe_2O_3^t$	13.81	10.73	13.56	9.79	14.45	14.50	14.39	14.13	14.19	11.80
MnO	0.18	0.13	0.16	0.13	0.26	0.14	0.13	0.13	0.11	0.12
MgO	7.03	5.35	5.26	5.41	10.38	10.44	9.75	9.74	8.67	6.19
CaO	10.15	10.28	10.31	10.31	12.31	12.84	13.23	12.47	13.83	10.85
Na_2O	2.25	2.23	2.45	2.26	1.73	1.43	1.39	1.17	0.93	2.02
K_2O	1.69	1.63	1.85	1.90	0.84	0.72	1.32	1.54	1.36	1.20
P_2O_5	0.56	0.56	0.67	0.60	0.56	0.56	0.59	0.60	0.59	0.57
LOI	1.24	4.40	3.38	2.16	1.72	2.12	1.78	2.19	3.19	3.19
Sum	96.21	99.05	98.61	100.33	98.00	98.69	99.28	98.25	96.54	98.59
Norm. qtz	–	4.77	–	6.65	–	–	–	–	–	5.21
Norm. ne	–	–	–	–	0.35	–	0.57	–	0.24	–
Trace elements (ppm)										
Sc	33.1	27.6	24.4	25.9	31.8	32.0	31.4	31.9	30.8	27.4
Cr	231	167	69	305	613	605	569	579	591	409
Co	49.0	42.9	42.4	38.9	62.5	62.2	59.6	60.9	60.5	43.6
Ni					259	261	246	247	288	159
Rb	43.8	33.7	35.7	38.6	11.1	7.7	22.3	29.0	23.2	36.4
Sr	113	825	1047	878	962	1012	964	744	975	911
Zr					314	343	312	428	331	331
Cs					3.65	0.18	0.19	0.16	0.42	0.34
Ba					497	535	601	616	729	636
La	62.0	64.8	72.9	66.6	61.9	60.4	64.1	61.9	64.8	68.7
Ce	155	146	173	150	130	129	136	136	140	138
Sm	14.9	14.2	16.6	13.8	13.9	14.1	14.2	14.1	13.9	12.9
Eu	4.0	3.8	4.5	4.0	3.9	3.9	4.0	4.0	4.1	3.8
Tb					1.34	1.37	1.27	1.35	1.23	1.23
Yb	2.6	2.6	3.1	2.4	2.5	2.7	2.6	3.1	3.0	2.8
Lu	0.36	0.29	0.37	0.30	0.28	0.21	0.25	0.26	0.27	0.32
Hf	10.2	9.3	10.5	9.5	10.3	10.0	10.4	10.6	9.9	9.0
Ta					5.73	5.53	5.81	5.83	5.92	4.73
Th	6.48	5.83	6.92	6.37	8.15	8.16	8.42	8.34	6.79	7.09
U	1.8	1.6	1.7	1.7	1.9	1.6	1.8	1.7	1.8	1.3
Pb		6.55	6.57							9.56

TABLE 1 (continued)

	Vestfold, Horten profile									
	CO F8b	CO F8c	CO F9	CO F10	CO F11	CO F12	Aph F13	Aph F14	Aph F15	Aph F16
Major elements (wt.%)										
SiO_2	46.48	45.47	47.44	46.40	45.34	45.81	44.31	44.90	44.32	44.85
TiO_2	4.36	4.24	4.63	4.35	4.68	4.91	4.81	4.68	4.85	4.79
Al_2O_3	9.58	8.72	10.69	9.32	10.65	10.20	9.46	9.23	9.60	9.55
$Fe_2O_3^t$	12.57	13.12	12.96	12.80	13.04	13.32	13.51	12.91	13.82	13.16
MnO	0.13	0.15	0.13	0.15	0.15	0.21	0.16	0.14	0.15	0.13
MgO	6.96	8.29	6.08	7.55	5.82	7.71	8.10	7.28	7.87	7.88
CaO	11.49	11.99	10.15	12.32	9.78	10.31	11.59	11.39	10.58	10.66
Na_2O	1.94	1.74	2.40	1.93	2.19	2.08	1.70	1.58	1.71	1.72
K_2O	1.63	1.42	2.03	1.45	2.00	1.74	1.92	2.20	1.91	2.14
P_2O_5	0.54	0.49	0.62	0.53	0.63	0.67	0.75	0.70	0.77	0.72
LOI	2.26	2.70	2.05	2.89	3.08	1.91	1.99	2.96	2.14	3.07
Sum	97.94	98.33	99.18	99.69	97.36	98.87	98.30	97.97	97.72	98.67
Norm. qtz	0.59	–	0.23	–	0.05	–	–	–	–	–
Norm. ne	–	–	–	–	–	–	–	–	–	–
Trace elements (ppm)										
Sc	29.8	27.3	31.2	31.9	24.6	27.5	29.8	28.9	29.9	28.3
Cr	472	417	465	465	367	352	404	359	383	394
Co	47.6	45.2	53.0	50.5	44.9	51.2	50.9	47.3	50.9	52.5
Ni	168	166	182	183	116	149	157	135	147	152
Rb	35.4	44.2	37.1	30.9	46.1	42.7	44.7	50.8	32.2	42.7
Sr	836	958	776	802	946	921	983	1150	1189	986
Zr	294	313	241	298	264	367	386	401	361	372
Cs	0.10	0.25	0.14	0.18	0.12	0.03	0.26	0.23	0.19	0.22
Ba	520	636	430	487	639	532	631	713	767	641
La	63.0	71.6	56.5	59.9	71.4	73.5	79.4	76.9	81.7	74.9
Ce	131	148	126	126	155	152	168	164	171	162
Sm	13.0	14.3	12.4	12.9	14.3	16.5	16.8	16.5	17.5	16.2
Eu	3.7	4.1	3.5	3.6	4.2	4.5	4.7	4.7	4.9	4.6
Tb	1.19	1.26	1.10	1.19	1.26	1.59	1.53	1.46	1.51	1.50
Yb	2.7	2.9	2.6	3.0	3.3	3.4	3.3	3.3	3.8	3.1
Lu	0.28	0.33	0.28	0.29	0.35	0.33	0.35	0.36	0.35	0.35
Hf	9.3	10.2	8.6	8.7	10.1	11.3	11.3	10.9	11.7	11.0
Ta	4.62	5.33	4.17	4.58	5.37	5.82	6.86	6.45	6.99	6.40
Th	6.44	7.52	6.14	6.47	7.97	7.08	8.15	8.08	8.67	7.83
U	1.6	2.5	1.6	1.0	1.3	2.1	1.6	2.3	2.3	2.1
Pb									6.38	5.88

$Fe_2O_3^t$ = total Fe as Fe_2O_3.

(To be continued)

The *P basaltic lavas* differ from the other porphyritic flows by carrying phenocrysts exclusively of plagioclase. The phenocrysts (5–8% of the rock volume) are up to 18 mm long and normally occur in aggregates consisting of up to 12 crystals. The groundmass is dominated by feldspar (60–70% of the rock volume), but also carries augite, pseudomorphs after olivine, apatite (2%) and magnetite$_{ss}$ (3%). Alteration and microlitic cavities as in CO basalt.

The *aphyric lavas* in the lower part of the sequence are mineralogically similar to the CO basalts, but are even-grained. Aphyric lavas occurring between PCO lavas are lighter coloured than

TABLE 1 (continued)

	Vestfold, Horten profile									
	Aph F17	PCO F18	POC F20	P F21	P F22	P F23	P F24	P F25	P F26	PCO FX0
Major elements (wt.%)										
SiO_2	44.50	46.55	46.61	49.17	50.77	49.63	50.43	52.21	48.22	47.56
TiO_2	4.82	2.59	2.87	3.39	3.50	3.23	3.29	3.30	3.36	2.30
Al_2O_3	9.28	14.55	15.06	17.07	17.40	16.70	16.64	16.46	16.52	10.22
$Fe_2O_3^t$	13.20	11.29	11.96	10.43	10.77	10.19	10.18	11.03	10.59	12.47
MnO	0.15	0.13	0.13	0.18	0.23	0.16	0.14	0.15	0.23	0.13
MgO	8.11	7.18	7.98	4.57	3.77	2.77	2.75	2.61	3.89	7.99
CaO	11.24	10.70	8.59	4.62	4.25	5.53	5.22	4.72	5.36	11.58
Na_2O	1.59	2.38	3.07	3.49	4.00	4.21	4.29	4.85	3.53	2.01
K_2O	1.78	1.59	1.67	4.29	4.55	4.13	4.16	3.65	3.73	1.24
P_2O_5	0.73	0.41	0.43	1.08	1.13	1.04	1.06	1.08	1.23	0.30
LOI	2.16	1.91	1.38	3.10	2.75	3.18	1.98	2.26	2.80	2.50
Sum	97.56	99.28	99.75	101.39	103.12	100.77	100.14	102.32	99.46	98.30
Norm. qtz	–	–	–	–	–	–	–	–	–	–
Norm. ne	–	–	1.61	–	0.12	3.81	2.5	4.37	–	–
Trace elements (ppm)										
Sc	29.5	22.5	25.5	9.1	9.1	8.9	8.9	8.6	8.9	44.1
Cr	429	174	193	36	21	25	19	27	20	320
Co	49.0	43.4	44.7	27.6	27.7	24.4	25.9	23.7	25.0	56.9
Ni	168	90	94	7	23	28	6	7	5	102
Rb	39.5	30.2	46.9	98.3	113	105	102	76.9	100	30.0
Sr	1084	996	1441	1615	1752	1649	1642	1461	1756	876
Zr	398	174	214	560	607	585	521	605	557	164
Cs	0.20	0.30	0.45	0.67	0.78	1.05	1.02	0.61	1.00	0.35
Ba	579	724	792	1490	1069	1010	1031	988	1160	471
La	76.5	42.0	45.6	143	132	132	132	129	134	34.4
Ce	161	85	105	275	257	259	271	256	257	68.4
Sm	16.3	7.6	8.6	24	24	23	24	23	24	7.3
Eu	4.7	2.4	2.5	7.1	7.1	6.8	7.2	6.8	6.8	2.2
Tb	1.46	0.75	0.81	2.11	2.04	2.08	2.12	1.97	2.11	0.83
Yb	3.5	2.2	1.5	4.0	4.1	3.7	4.2	3.9	4.0	2.5
Lu	0.36	0.23	0.25	0.53	0.55	0.49	0.49	0.43	0.49	0.38
Hf	10.6	5.0	5.1	15.0	15.0	14.2	14.5	14.4	14.2	4.6
Ta	6.39	2.99	3.13	10.3	10.2	9.9	10.1	10.2	10.1	2.78
Th	8.08	4.00	4.25	13.1	13.8	12.7	13.6	13.4	13.1	3.23
U	1.4	0.94	0.72	2.9	4.0	3.6	3.7	4.7	2.7	0.91
Pb				9.17		7.89				

those in the lower part of the section; plagioclase makes up more than 60% of their volume. Alteration and miarolitic cavities as in CO basalts.

The petrographic observations in CO and CPO lavas are in agreement with the crystallization sequence:

ol → cpx → mt_{ss} → plag → ap.

Basaltic lava, Krokskogen

The single B_1 flow at the base of the lava sequence at Krokskogen carries microphenocrysts of plagioclase in an aphanitic groundmass consisting of plagioclase, augite and Fe–Ti-oxides. Alter-

TABLE 1 (continued)

	Vestfold, Horten profile								
	PCO FX1	PCO FX2	PCO FX3	PCO FX4	Aph FZ1	PCO FZ2	PCO FZ3	PCO FZ4	PCO FZ5
Major elements (wt.%)									
SiO_2	47.90	50.33	46.33	47.48	47.30	47.30			
TiO_2	2.75	2.97	2.93	2.93	2.97	2.95			
Al_2O_3	12.98	14.04	11.18	14.84	13.70	12.82			
$Fe_2O_3^t$	12.83	11.26	12.81	12.78	12.39	13.75			
MnO	0.12	0.18	0.17	0.17	0.20	0.26			
MgO	5.17	4.07	6.70	5.37	3.88	7.29			
CaO	10.36	9.22	9.57	7.07	6.50	10.18			
Na_2O	2.79	3.25	2.59	2.64	5.44	2.42			
K_2O	1.61	2.08	3.12	3.78	1.51	1.30			
P_2O_5	0.48	0.52	0.48	0.59	0.53	0.25			
LOI	1.72	1.65	2.32	2.16	4.77	2.46			
Sum	98.71	99.57	98.20	99.81	99.19	100.98			
Norm. qtz	0.27	–	–	–	–	–			
Norm. ne	–	–	2.22	0.21	3.15	–			
Trace elements (ppm)									
Sc	25.8	24.7	37.2	18.5	21.8	31.5	30.7	32.6	25.5
Cr	130	50	119	34	23	195	190	186	108
Co	48.5	36.6	47.8	44.0	35.8	53.6	52.6	55.0	42.1
Ni	55	32	57		1	81	81		60 31
Rb	37.4	44.9	78.6	94.5	22.0	25.1	55.7	38.9	33.2
Sr	866	982	1121	1266	844	656	751	737	651
Zr	236	247	303		304	155	176	261	280
Cs	0.19	0.28	0.78		0.12	1.78	1.87	0.87	0.67
Ba	652	811	1037		640	510	709	843	558
La	53.1	61.4	47.9	52.0	58.9	40.2	39.7	48.8	59.0
Ce	105	121	96	104	115	83.4	81	97.8	111
Sm	9.6	11.8	10.9	10.7	10.9	8.9	8.7	10.0	12.2
Eu	2.7	3.2	2.9	2.9	2.9	2.6	2.5	2.8	3.2
Tb	1.00	1.22	1.11		1.07	0.90	0.90	1.07	1.30
Yb	2.4	3.1	2.8	2.6	3.1	2.7	2.6	2.8	3.6
Lu	0.38	0.43	0.38	0.39	0.41	0.41	0.35	0.33	0.54
Hf	6.3	8.2	7.2	6.5	6.8	5.1	4.9	6.3	8.1
Ta	3.46	3.84	3.40		4.26	2.91	2.97	3.84	4.17
Th	4.80	6.18	4.05	5.28	6.63	3.45	3.36	4.87	5.46
U	1.3	1.6	1.3	1.3	2.9	0.89	1.1	1.2	2.2
Pb		7.25				4.57			

$Fe_2O_3^t$ = total Fe as Fe_2O_3.

(To be continued)

ation products are epidote, chlorite, actinolite and calcite. Calcite also occur in vesicles.

Analytical methods

All analyses were performed at the Mineralogisk-Geologisk Museum, University of Oslo.

Major and trace element analyses

Whole-rock samples were analyzed for major elements using XRF on fused pellets. The trace elements Cr, Ni, Rb, Sr, Y and Zr were analyzed by XRF on pressed powder pellets. All XRF analyses were performed in duplicate and

TABLE 1 (continued)

	Vestfold, Holmestrand profile							Krokskogen
	CO OB102	PCO OB101	PCO OB100	PCO OB99	PCO OB98	PCO OB97	CO OB96	Aph OB87
Major elements (wt.%)								
SiO_2	46.06	44.51	45.30	45.03	47.78	47.95	47.16	48.58
TiO_2	4.48	3.03	4.66	3.36	3.26	2.45	2.44	2.47
Al_2O_3	7.55	12.87	10.03	8.12	9.38	16.05	11.21	13.52
$Fe_2O_3^t$	14.23	13.25	14.78	15.11	14.14	11.51	13.81	14.47
MnO	0.16	0.20	0.20	0.19	0.19	0.16	0.28	0.16
MgO	11.71	9.18	7.49	11.40	9.18	5.83	8.30	7.52
CaO	10.71	11.38	10.97	11.84	10.88	8.71	11.91	8.27
Na_2O	1.34	2.31	2.11	1.53	2.30	3.74	2.35	2.28
K_2O	1.29	1.14	1.94	1.61	1.72	1.99	1.12	0.85
P_2O_5	0.50	0.58	0.72	0.58	0.60	0.48	0.42	0.39
LOI	0.89	0.28	0.50					
Sum	98.92	98.73	98.70	98.77	99.43	98.87	99.00	98.51
Norm. qtz	–	–	–	–	–	–	–	1.68
Norm. ne	0.43	2.21	–	0.19	–	3.61	–	–
Trace elements (ppm)								
Sc	33.2	23.2	27.2	32.9	28.2	18.5	43.3	29.2
Cr	876	330	403	769	551	111	304	125
Co	44.5	54.7	56.7	67.7	60.0	41.2	55.0	46.0
Ni	262	68	149	275	163	34	57	65
Rb	24.8	14.5	45.0	28.7	28.5	62.9	18.2	27.1
Sr	174	2390	1002	921	778	1452	573	691
Y	26.8	19.4	41.1	30.9	36.1	20.6	30.4	
Zr	282	218	402	252	283	201	179	162
Sb	0.11	0.15	0.13	0.13	0.15	0.06	0.02	
Cs	0.48	1.31	0.25	0.43	0.24	1.68	2.49	1.03
Ba	438	1139	410	439	447	556	326	397
La	58.0	60.8	79.1	59.7	58.0	44.0	36.4	24.2
Ce	117.7	105.7	148.4	110.8	110	82.4	72.8	45.2
Sm	10.9	9.5	16.4	11.1	9.8	7.1	7.9	7.7
Eu	3.3	2.9	4.4	3.5	3.2	2.3	2.3	2.2
Tb	1.03	0.86	1.39	1.03	1.15	0.76	0.88	1.32
Dy	6.3	4.3	8.0	5.7	6.5	4.5		4.7
Yb	1.9	1.1	2.3	2.2	1.9	1.4	2.1	2.8
Lu	0.25	0.18	0.36	0.27	0.27	0.22	0.33	0.39
Hf	9.8	7.5	10.8	9.8	9.9	6.7	5.7	5.8
Ta	4.62	4.51	4.62	4.38	4.37	3.05	2.58	0.95
Th	6.09	4.82	8.05	5.06	6.35	4.29	3.06	2.01
U	2.0	1.5	1.5	0.90	2.1	1.2	0.85	0.47
Pb								5.24

$Fe_2O_3^t$ = total Fe as Fe_2O_3.

calibrated against recommended values for international standards as given by Govindaraju (1984). Th and U were determined by natural gamma-ray radiation on 0.5 kg crushed samples using a Ge(Li) detector. Other trace elements were analyzed using instrumental NAA following methods described by Gordon et al. (1968) and Brunfelt and Steinnes (1969). Rb, Sr, Sm and Nd were also determined by isotope dilution analysis (see below).

For XRF, precision of analyses was estimated

TABLE 2

Precision of analyses at the 1σ level of confidence

Rb, Sr (at 100 ppm), Sc, Zr, Ni	⩽ ±1%
Mn, Cr	⩽ ±2%
P (at 0.4 wt.%), La, Tb, Ta, Th	±3%
Co, Ba, Ce, Sm, Eu, Hf	±5%
U	±8%
Cs, Lu, Yb	±18–20%

on the basis of pooled variance of samples analyzed in duplicates. For INAA, precision was determined by 3–8 counts of the BCR-1 standard. Estimated precisions for major elements are ⩽ 1% (at the 1σ confidence level), and those for trace and minor elements are listed in Table 2.

Sm–Nd and Rb–Sr isotope analyses

The chemistry and mass spectrometry procedures have been described by Mearns (1986). Laboratory total system blanks are typically ≪ 1 ng for both Nd and Sr and are thus negligible for this study. Blank concentrations were measured by isotope dilution using mixed ^{87}Rb–^{84}Sr and ^{149}Sm–^{148}Nd spikes.

Isotopic ratios were measured on a VG 354 fully automated 5-collector instrument. Laboratory values for standards are BCR-1 (13 duplicate analyses): $^{147}Sm/^{144}Nd = 0.1384 \pm 2$, $^{143}Nd/^{144}Nd = 0.512650 \pm 20$ and $^{145}Nd/^{144}Nd = 0.348395 \pm 28$ (all 2σ mean). Nd isotopic ratios are normalized to $^{146}Nd/^{144}Nd = 0.721900$. Twenty single analyses of Johnson and Matthey Nd_2O_3, batch no. S819093A: $^{143}ND/^{144}Nd = 0.511125 \pm 8$ and $^{145}Nd/^{144}Nd = 0.348412 \pm 8$ (2σ mean). 30 single analyses of NBS 987: $^{87}Sr/^{86}Sr$: 0.710227 ± 21 (2σ mean).

The decay constant used for $^{147}Sm = 6.54 \times 10^{-12}$ y^{-1}. ε_{Nd} and ε_{Sr} values are calculated relative to CHUR with present-day $^{147}Sm/^{144}Nd = 0.1967$, $^{143}Nd/^{144}Nd = 0.512647$, $^{87}Rb/^{86}Sr = 0.0827$, and $^{87}Sr/^{86}Sr = 0.7045$ (Allègre et al., 1983; Jacobsen and Wasserburg, 1984), using Rb–Sr ages to correct for in situ radiogenic ^{143}Nd.

Major and trace element relations

Effects of alteration

Relatively high LOI (1.2–4.8%; Table 1) in the Vestfold lavas reflects low-temperature alteration. The presence of calcite and K-bearing secondary minerals (sericite, biotite), as well as considerable variations in K_2O/Na_2O ratios among samples which are otherwise compositionally similar, suggests that alkalies and calcium were mobilized by alteration processes. However, like other Oslo Rift magmatic rocks, the majority of the Vestfold basaltic lavas have K_2O/Na_2O close to 1 and are thus potassic in nature.

Trace elements considered to be strongly incompatible during partial melting and crystallization in basaltic systems fall into two groups. One group, including Ta, Th, La, Sm, Hf and Zr, shows a restricted range in element–element ratios (Table 3, Fig. 2). The elements Cs and Rb, in contrast, resemble K by showing considerable variations among lavas which are compositionally similar with respect to other elements (e.g., F13–F17 in Table 3). Also U shows some scatter. High concentrations of Sr relative to Th in the PCO basalts (Fig. 3) have been assigned to accumulation of feldspar (see below). However, also the CO basalts exhibit considerable variations in Sr/Th ratios, samples FA1 and OB102 are strongly depleted in Sr relative to the other samples (Table 1).

TABLE 3

Average ratios and standard deviations for selected pairs of incompatible elements in basaltic lavas from Vestfold. Data in Table 1

	Average ± 1σ	Percentage	Number of samples
Th/Ta	1.33 ± 0.14	10	41
Sm/La	0.20 ± 0.02	10	41
Th/La	0.103 ± 0.012	12	41
Sm/Zr	0.0434 ± 0.0050	12	41
Hf/Zr	0.0286 ± 0.0037	13	46
P/Zr	8.5 ± 1.9	22	38
U/Th	0.258 ± 0.059	23	46
K/Th	2420 ± 1100	45	36
Rb/Th	6.7 ± 3.8	56	46
Cs/Th	0.12 ± 0.17	140	41

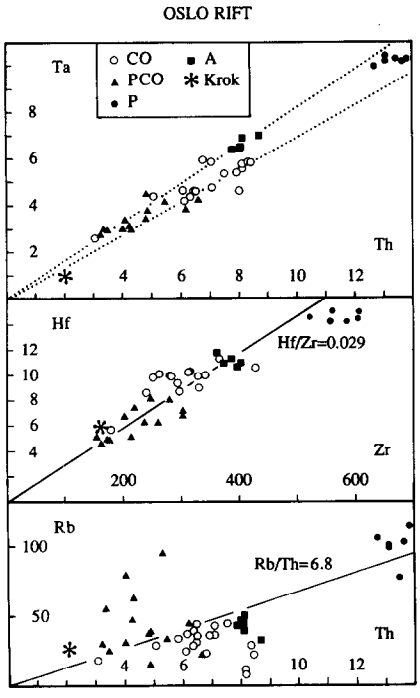

Fig. 2. Relationships between lithophile elements (given in ppm) in basaltic lavas (B_1) from Vestfold and Krokskogen. *C* = clinopyroxene; *O* = olivine; *P* = plagioclase phenocrysts; *A* = aphyric; *Krok* = aphyric basalt from Krokskogen. Regression lines are fully drawn. The existence of two groups is suggested by dotted lines in the Ta–Th diagram.

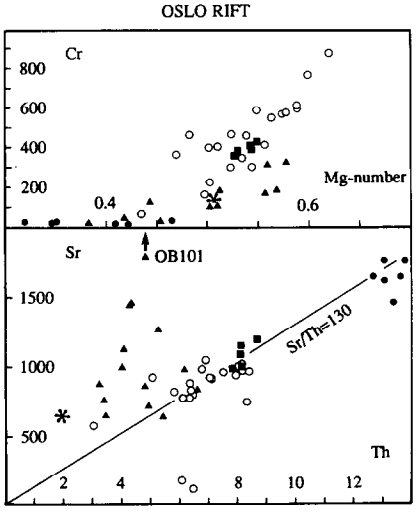

Fig. 3. (a) Cr–*Mg*-number and (b) Sr–Th relations among basaltic lavas (B_1) from Vestfold (open circles: cpx–ol (CO), triangles: plag–cpx–ol (PCO): closed circles: plag (P), squares: aphyric) and Krokskogen (star). (Cr, Sr and Th in ppm, *Mg*-number = cation proportions $Mg/(Mg + Fe_{total})$).

This suggests that some of the observed variations in Sr relative to other elements may result from alteration. Studies of interaction between basalts and fluids confirm that the elements Ca, K, Cs, Rb, Sr and U are readily affected by secondary processes such as hydrothermal activity and weathering (e.g., Hendersen, 1982).

Compositional character of B_1 basalts in Vestfold and Krokskogen

The petrographic differences between the lower and the upper parts of the Vestfold lava sequence are reflected in compositional differences. CO and aphyric basalts in the lower part of the profiles (Table 1) are relatively Ti-rich ($TiO_2 \leqslant 5.4$ wt.%); MgO ranges from 5.3 to 11.7 wt.%. Most of these lavas are ol–opx normative or show insignificant amounts of normative qtz or ne; three samples have more than 5% normative qtz.

The younger PCO and P lavas (F18–FZ2) have a more "evolved" character (MgO = 2.6–8.0%). Six of fifteen samples in the Horten profile have significant amounts of normative nepheline (1.6–4.4%); significant normative qtz is not found (Table 1).

The majority of the lavas in the lower part of the profile are subalkaline basalts (TAS classification). The most Mg–Ca-rich samples, F1–F6, classify as picrobasalts, but their high proportions of augite phenocrysts suggest that their ultrabasic nature is due to accumulation of clinopyroxene rather than a property of the melt. The PCO lavas classify as subalkaline to alkaline basalts and potassic trachybasalts, the P lavas as shoshonites.

The *Vestfold basaltic lavas* show large variations in both compatible and incompatible trace element concentrations (e.g., Sc = 8.6–44.1 ppm; Sr = 110–2390 ppm; Th = 3.1–14.0 ppm; Table 1). The highest concentrations of incompatible elements and Sr are found in the P lavas. Sc, Cr, Co and Ni correlate roughly with *Mg*-number (Fig. 3). The majority of the CO basalts and the aphyric basalts have relatively constant Sr/Th of about 130 (Fig. 3). The P lavas have similar Sr/Th ratios (109–133), whereas most of the PCO basalts have high and highly variable Sr/Th ratios (125–496).

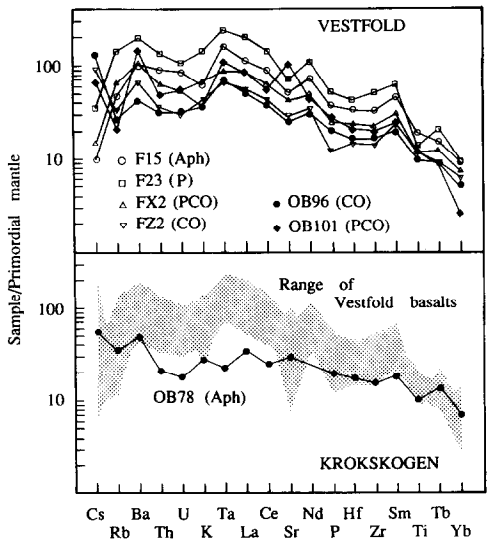

Fig. 4. Representative trace element enrichment patterns for basaltic lavas (B_1) from Vestfold and Krokskogen in the Oslo Rift. Concentrations are normalized by division with respective concentrations in the primordial mantle given by Wood (1979). Phenocrysts are indicated in parentheses; *P* = plagioclase, *C* = clinopyroxene, *O* = olivine, *Aph* = aphyric.

The single, aphyric B_1 flow at *Krokskogen*, northwest of Oslo, is a subalkaline basalt with *Mg*-number of about 0.5. Some compositional variations have been observed between different exposures, particularly in Na_2O and K_2O. A representative major and trace element analysis is presented in Table 1.

Representative trace element enrichment patterns normalized to the primordial mantle (Wood, 1979) are shown in Fig. 4. The Vestfold basaltic lavas have uniform patterns characterized by a marked enrichment in strongly relative to moderately incompatible elements, and positive Ta anomalies. The PCO lavas tend to be enriched in Ba and Sr relative to the other petrographic types. The B_1 basalt at Krokskogen shows a less marked difference in enrichment between strongly and moderately lithophile elements than do the other basaltic rocks, and has no positive Ta anomaly (Fig. 4).

Strongly incompatible elements which have not been affected by alteration processes show small but significant ranges in element–element ratios (Table 3, Fig. 2). The Krokskogen basalt tends to define the upper or lower limit in each range. In the Ta–Th diagram, the Vestfold basalts may be roughly divided into two groups with slightly different Ta/Th ratios, each group shows a range in Ta and Th concentrations. There is no simple correlation between Th/Ta ratio and petrography or stratigraphic position.

Fractional crystallization / accumulation

Some of the observed variations in trace element relations correspond to those to be expected from fractional crystallization and/or accumulation of the observed phenocryst phases (ol, cpx, mt, plag): large variations in concentrations but similar ratios between lithophile elements expected to have similar bulk distribution coefficients during crystallization of the observed phenocryst phases (Fig. 2, Table 3); decreasing, and variable concentrations of Cr, Sc, Ni and Co with decreasing *Mg*-number; high and variable Sr/Th ratios in lavas which are rich in plagioclase phenocrysts (PCO in Table 1; Fig. 3).

The P lavas have very low concentrations of Sc, Cr, Co and Ni (Table 1, Fig. 2), although they do not carry phenocrysts of ol or cpx. Furthermore, they are the most highly enriched in incompatible elements of all the lavas and have similar Sr/Th ratios to the more magnesian aphyric basalts in the lower part of the Horten profile (118–140 and 109–134, respectively) (Fig. 3). This strongly suggests that also the parent magma of the P lavas had a history of extensive removal of ol + cpx before eruption, whereas removal of plagioclase appears to have been insignificant.

However, the observed scatter in incompatible element ratios, as well as the tendency for the samples to define two trends of constant Th/Ta ratios, suggest that processes other than fractional crystallization/accumulation have been in operation as well.

Isotopic compositions

The isotopic composition of whole rock samples of B_1 basaltic lavas from Vestfold and Krokskogen is given in Table 4 and plotted in Figs. 5 and 6.

TABLE 4

Isotopic relations among basaltic lavas from Vestfold and Krokskogen in the southern and central part of the Oslo Region.

Sample	Rb (ppm)	Sr (ppm)	$^{87}Rb/^{86}Sr$	$^{87}Sr/^{86}Sr \pm 1\sigma$	Sm (ppm)	Nd (ppm)	$^{147}Sm/^{144}Nd$	$^{143}Nd/^{144}Nd \pm 1\sigma$	ε_{Sr}	ε_{Nd}
Vestfold, Horten profile										
FA2 [a]	33.7	825	0.1183	0.704580 ± 16	13.8	73.2	0.1149	0.512595 ± 4	−1.0	+2.1
FA3 [a]	35.7	1047	0.0985	0.704514 ± 14	16.4	87.3	0.1142	0.512606 ± 4	−0.7	+2.4
F1	10.7	907	0.0340	0.704022 ± 8	14.3	74.9	0.1163	0.512544 ± 3	−3.8	+3.0
F4	28.2	721	0.1131	0.704505 ± 7	14.5	76.0	0.1162	0.512618 ± 9	−1.8	+2.5
F6	22.7	937	0.06993	0.704073 ± 7	14.5	77.9	0.1134	0.512606 ± 3	−5.3	+2.4
F8A [a]	36.4	911	0.1156	0.705061 ± 10	13.5	74.8	0.1096	0.512552 ± 6	+6.0	+1.5
F8b	34.0	799	0.1231	0.705052 ± 8	13.4	72.6	0.1124	0.512570 ± 5	+5.4	+1.7
F8c	43.4	916	0.1372	0.705091 ± 7	14.4	79.7	0.1101	0.512595 ± 20	+5.1	+2.3
F9	34.7	709	0.1414	0.705129 ± 10	12.8	68.6	0.1139	0.512549 ± 3	+5.4	+1.3
F10	29.6	752	0.1140	0.705039 ± 7	13.2	70.9	0.1132	0.512549 ± 6	+5.8	+1.3
F11	44.7	902	0.1432	0.705204 ± 9	14.5	81.1	0.1091	0.512507 ± 2	+6.3	+0.62
F12	39.6	871	0.1317	0.704460 ± 8	16.6	87.9	0.1151	0.512595 ± 3	−3.5	+2.1
F13	42.9	1131	0.1097	0.703871 ± 9	17.0	92.6	0.1121	0.512665 ± 3	−10.6	+3.6
F14	48.7	1084	0.1302	0.704144 ± 7	16.7	89.5	0.1134	0.512641 ± 3	−7.9	+3.1
F15 [a]	32.2	1189	0.0783	0.704037 ± 10	17.7	96.1	0.1120	0.512689 ± 6	−6.3	+4.1
F16 [a]	42.7	986	0.1254	0.704364 ± 10	16.5	88.8	0.1129	0.512689 ± 5	−4.5	+4.0
F17	38.1	1035	0.1066	0.703940 ± 9	17.0	91.6	0.1126	0.512656 ± 3	−9.4	+3.4
F18	29.3	948	0.0839	0.703963 ± 10	8.0	44.1	0.1102	0.512621 ± 3	−7.7	+2.8
F21 [a]	98.3	1615	0.1762	0.704736 ± 10	24.8	144.9	0.1043	0.512631 ± 6	−2.3	+3.2
F22	112.9	1693	0.1929	0.704810 ± 30	24.7	140.1	0.1073	0.512577 ± 4	−2.3	+2.1
F23 [a]	104.9	1649	0.1844	0.704770 ± 10	23.5	136.1	0.1051	0.512616 ± 5	−2.3	+2.9
F24	106.6	1591	0.1937	0.704745 ± 8	24.1	138.7	0.1059	0.512614 ± 2	−3.3	+2.8
F26	101.7	1704	0.1726	0.704550 ± 30	24.0	140.2	0.1045	0.512582 ± 9	−4.7	+2.3
FX2 [a]	44.9	982	0.1321	0.705143 ± 10	11.6	63.5	0.1117	0.512522 ± 9	+6.1	+0.8
FZ2 [a]	22.8	656	0.1005	0.704315 ± 10	8.7	45.1	0.1171	0.51267 ± 6	−3.7	+3.5
Vestfold, Holmestrand profile										
OB102	24.8	174	0.3992	0.70653 ± 8					+9.6	
OB101 [b]	14.5	2393	0.0175	0.70571 ± 7	9.5	57.8	0.0995	0.511813 ± 15	+21.0	+2.9
OB100	45.0	1002	0.1299	0.70451 ± 3	16.4	90.0	0.1112	0.512610 ± 5	−2.7	+2.6
OB99	28.7	921	0.0901	0.70492 ± 3	11.1	60.9	0.1105	0.512648 ± 7	+5.5	+3.3
OB98	28.5	778	0.1070	0.70496 ± 8					+5.1	
OB97	62.9	1452	0.1244	0.70490 ± 6					+3.2	
OB96	18.2	573	0.0921	0.70433 ± 3	7.9	40.5	0.1182	0.512695 ± 4	−3.0	+3.9
Krokskogen										
OB8 [a]	13.0	372	0.1012	0.70572 ± 5					+16.2	
OB87 [b]									+18.0	−0.7

[a] Neumann et al. (1988b);
[b] Jacobsen and Wasserburg (1978) and this work.

The Horten basaltic rocks do not show any correlation $^{87}Rb/^{86}Sr$–$^{87}Sr/^{86}Sr$ or $^{147}Sm/^{144}Nd$ –$^{143}Nd/^{144}Nd$ (Table 4). However, they define a mixing trend with respect to ε_{Nd} and ε_{Sr} (300 Ma) from about (+4, −10) to about (+0.5, +6). The high ε_{Nd} end of the mixing trend is defined by aphyric basalts, the low end by CO basalts and the PCO lava FX2. The Krokskogen basalt falls in the low-ε_{Nd} continuation of this mixing trend.

Some scatter about the mixing trend is probably caused by secondary processes which have clearly affected Rb, probably also Sr. Two of the Holmestrand basaltic lavas (the strongly altered OB101 analyzed by Jacobsen and Wasserburg,

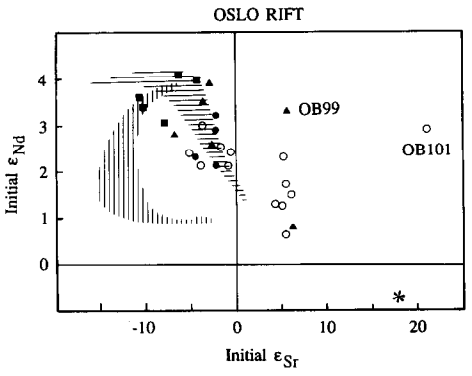

Fig. 5. Initial ε_{Nd}–ε_{Sr} relations (300 Ma) among basaltic lavas (B_1) from Vestfold (open circles: cpx–ol phenocrysts (CO), triangles: plag–cpx–ol (PCO): closed circles: plag (P), squares: aphyric) and Krokskogen (star). Vertically hatched area: range of alkaline basalts from the Skien area (Anthony et al., 1989); horizontally hatched area: range of trachyandesitic intrusive and extrusive rocks (larvikites and rhomb-porphyry lavas). Data from Neumann et al. (1988b) and this work.

1978; and OB99) which fall to the high ε_{Sr} side of the main trend are heavily altered. Sample OB101 is very rich in Sr (2390 ppm) and strongly depleted in Rb relative to other strongly incompatible elements (e.g., Th, Ta; Table 1). The estimated high initial ε_{Sr} of this sample is probably the result of addition of Sr and/or loss of Rb during alteration.

There is no correlation between initial isotopic ratios and Sm/Nd, 1/Nd, Rb/Sr or 1/Sr or incompatible element concentrations. There is, however, a tendency for lavas with low ε_{Nd} to be qtz-normative, or have only small amounts of normative ol. These observations support the earlier suggestion that a combination of processes have been in operation.

Data from Neumann et al. (1988b) show that the Horten and Krokskogen samples also define linear trends in the U–Pb and Th–Pb isotopic systems (Fig. 6). The slopes of these trends correspond to ages of roughly 500 and 600 Ma. Since an upper age of about 300 Ma is firmly established for the Oslo Rift (Sundvoll and Larsen, 1982; Sundvoll et al., 1990), the trends in Fig. 6 must consequently represent mixing trends, not isochrons. The highest Pb isotopic ratios are found for those samples which are most depleted with respect to Nd and Sr isotopes.

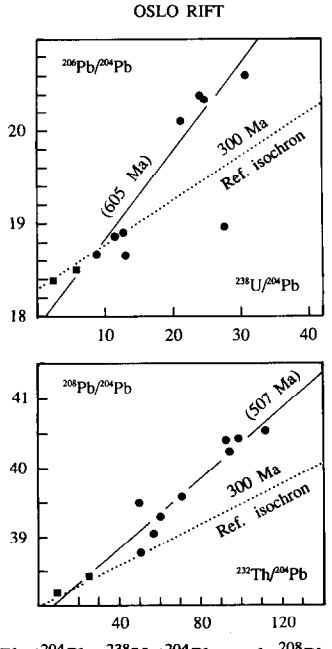

Fig. 6. $^{206}Pb/^{204}Pb$–$^{238}U/^{204}Pb$ and $^{208}Pb/^{204}Pb$–$^{232}Th/^{204}Pb$ relations among basalts from Horten, Vestfold (dots) and Krokskogen (squares). Data from Neumann et al. (1988b).

Discussion

The observed petrographic and chemical variations in the Vestfold basalts suggest the combined effects of different processes.

Mixing relations

The mixing trends defined by the majority of the basaltic lavas in the Sr–Nd and U–Th–Pb isotopic systems (Figs. 5, 6) require the involvement of (at least) two isotopically distinct sources. One is characterized by (ε_{Nd}, ε_{Sr}, $^{206}Pb/^{204}Pb$) (300 Ma) ($\geq +4$, ≤ -5, ≥ 19.2), the other by (≥ -1, $\geq +18$, ≤ 17.7). Neumann et al. (1988b) proposed that these isotopically distinct sources correspond to a mildly depleted mantle source and the lower crust, respectively.

There is increasing evidence of compositional heterogeneities in the mantle. Existing isotopic data world-wide require the existence of four "end-member" components (DMM = depleted MORB mantle, HIMU = high U/Pb, EM I and EM II = enriched mantle I and II) and are con-

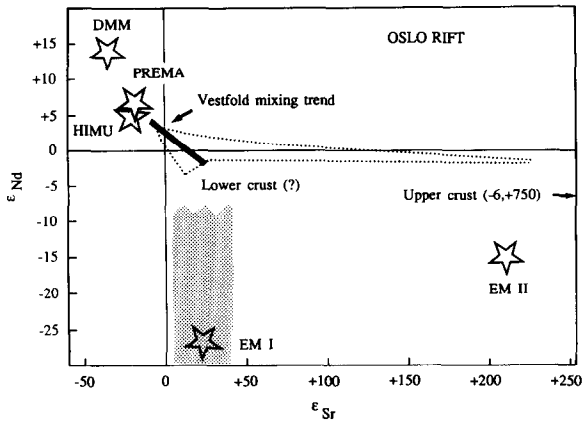

Fig. 7. Initial ε_{Nd}–ε_{Sr} relations among Permo-Carboniferous Oslo Rift rocks compared to principal mantle components at $t = 0$ Ma (stars) (Hart et al., 1986; Wörner et al., 1986; Zindler and Hart, 1986): DMM (depleted MORB mantle), PREMA (prevalent mantle), HIMU (high U/Pb), EM I and EM II (enriched mantle). Heavy line: Vestfold mixing trend; area enclosed by dotted line: range of single silicic samples; column: range of initial ratios among silicic intrusions which define isochrons in the Rb–Sr system. Data on the Oslo Rift from Neumann et al. (1988a, b), on the upper crust under southeastern Norway (recalculated to 300 Ma) (Andersen, 1987; Andersen and Taylor, 1988; A. Bjørlykke, pers. commun., 1988).

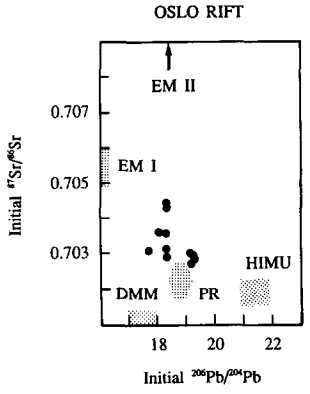

Fig. 8. Initial $^{206}Pb/^{204}Pb$–$^{87}Sr/^{86}Sr$ relations among Vestfold basaltic rocks compared to various mantle and crustal components. DMM, PR (= PREMA), HIMU, EM I and EM II are principal mantle components as given by Hart et al. (1986), Wörner et al. (1986) and Zindler and Hart (1986).

sistent with the existence of (at least) two additional components (PREMA = prevalent mantle, BSE = bulk silicate Earth) (Hart et al., 1986; Wörner et al., 1986; Zindler and Hart, 1986). The isotopic characteristics of most of these components are indicated in Figs. 7 and 8. These mantle heterogeneities mean that it is also possible to explain the isotopic relations among the Oslo Rift basalts in terms of mixing between depleted and enriched mantle components (e.g., PREMA–EM I–EM II in Figs. 7 and 8). A third possibility is various degrees of contamination of all the lavas.

Ratios between strongly incompatible elements may be effective in distinguishing between mantle and crustal sources. Ta and Nb are depleted relative to other strongly incompatible elements in the continental crust, and enriched in the mantle sources of MORB and OIB (Sun, 1980; Hofmann et al., 1986). Hofmann et al. (1986) proposed the use of the ratio Nb/U as a means of distinguishing.

Since Nb data are not available, we have chosen the ratio Th/Ta as the main basis for distinguishing mantle from crustal influence in this study (plotted against Th/La in Fig. 9). Average Th/Ta and Th/La for MORB (normal and enriched) and OIB are from Sun (1980) and Hofmann (1988). Data on different parts of the continental crust are from Weaver and Tarney (1984) and Taylor and McLennan (1985).

The Vestfold basaltic lavas show a restricted range in Th/Ta and Th/La (Fig. 9). A large group of lavas have Th/Ta within the range of MORB and OIB (0.9–1.2), and the rest have Th/Ta between those characteristic of the mantle and the lower crust. The highest Th/Ta is found for the Krokskogen basalt (2.1). The majority of the basaltic lavas have Th/La close to 0.10, i.e., similar to OIB and the lower crust. Four samples

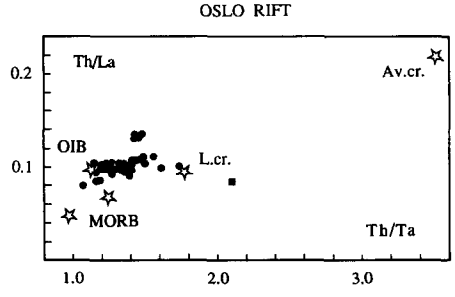

Fig. 9. Th/La–Th/Ta relations in basaltic lavas from the Oslo Rift (closed circles) compared to average values (stars) for MORB, OIB, lower crust (*L.cr.*) and average crust (*Av.cr.*), as given by Sun (1980), Weaver and Tarney (1984) and Taylor and McLennan (1985).

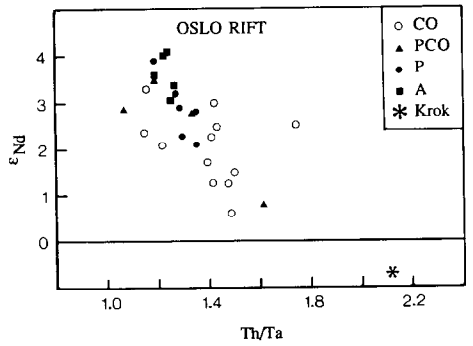

Fig. 10. Initial ε_{Nd}–Th/Ta relations among basaltic lavas (B_1) from Vestfold (open circles: cpx–ol phenocrysts (CO), triangles: plag–cpx–ol (PCO): closed circles: plag (P), squares: aphyric) and Krokskogen (star) in the Oslo Rift.

(F1–F4) have slightly higher Th/La (0.13). Increasing Th/Ta ratios are accompanied by decreases in ε_{Nd}, $^{206}Pb/^{204}Pb$ and $^{208}Pb/^{204}Pb$ (Fig. 10). Like the ε_{Nd}–ε_{Sr} relations, the ε_{Nd}–Th/Ta ones are less clear for the Holmestrand than for the Horten basalts.

The described trace element relations imply that a group of Vestfold basalts are uncontaminated, and have retained the chemical characteristics of their mantle source. The isotopic composition of this source is probably similar to the mantle component PREMA (prevalent mantle) for Permo-Carboniferous time (Figs. 7–9). PREMA ($t = 0$: $^{143}Nd/^{144} \approx 0.513$ ($\varepsilon = +6.9$), $^{87}Sr/^{86}Sr \approx 0.7032$ ($\varepsilon = -18.5$), $^{206}Pb/^{204}Pb \approx 18.8$) appears to represent an end-member for continental basalts in general (Wörner et al., 1986; Zindler and Hart, 1986). The Vestfold mantle source will be referred to as "PREMA".

The rest of the samples have higher Th/Ta ratios and lower initial ε_{Nd} which strongly suggests that a lower crustal component is involved. The isotopic composition of the most contaminated lava (Krokskogen) is about (−1, +18, +17.7); that of the lower crustal component must lie along the extension of the mixing trend towards lower ε_{Nd}. An isotopic model for the upper crust, based on a composite of Precambrian rocks west of the Oslo Region, gives (recalculated to 300 Ma): $\varepsilon_{Nd} = -6$, $\varepsilon_{Sr} = +750$, $^{206}Pb/^{204}Pb = 20.5$ (Andersen, 1987; Andersen and Taylor, 1988; A. Bjørlykke, personal communication, 1988).

The trace element data thus support contamination of magmas derived from mildly depleted mantle by lower crust (Neumann et al., 1988b). A crustal component is also in agreement with the observed tendency for lavas with low initial Nd isotopic ratios to be qtz-normative. Variations in incompatible element ratios and initial isotope ratios are not related to variations in trace element concentrations (e.g., Fig. 2). Contamination in the lower crust was consequently accompanied by, or followed by, processes which affect element concentrations, but do not fractionate strongly incompatible elements relative to one another, for example fractional crystallization and accumulation.

Mantle sources: evidence from other rock series

Mixing relations similar to those described for the Vestfold basalts ("PREMA"–lower crust) are also found for rocks in other parts of the Oslo Rift (Figs. 5, 7):

— Intrusive and extrusive rocks of trachyandesitic composition (larvikites and rhomb-porphyry lavas) from the southern and central part of the Oslo graben fall along the Vestfold ε_{Nd}–ε_{Sr} mixing trend. The most depleted sample has the composition (+4.2, −8.0, +19.3) (277 Ma) (Neumann et al., 1988b).

— A relatively young basalt (within the RP sequence) from Krokskogen carries olivine–clinopyroxenite xenoliths. The host basalt gives ε_{Nd}–ε_{Sr} of ($+4.16 \pm 0.17$, -5.5 ± 0.26) (275 ± 5 Ma). Acid-washed separates of clinopyroxene from two of the xenoliths give (+1.9, −1.1) and (+2.6, +1.8) (Neumann et al., 1988a).

— B_1 basaltic lavas in the Skien area in the southwestern part of the Oslo Graben cover a range in ε_{Nd}–ε_{Sr} values (Anthony et al., 1989). Nephelinites at the base of the lava sequence plot close to the HIMU–EM I mixing line of Zindler and Hart (1986) (+1.1 to +1.4, −13 to −15). Upwards in the section, ε_{Nd} increases with decreasing alkalinity towards that of uncontaminated Vestfold basalts. Anthony et al. (1989) proposed that the early part of the Skien magmatism tapped a reservoir with HIMU–EM I characteristics, which, with time, was overwhelmed by

magmas originating in a "PREMA" reservoir.

A "PREMA"-type mantle source thus appears to have been available under the northern and central part of the Oslo Rift. A source of similar composition (+4, −16) gave rise to the 540 Ma old carbonatitic rocks of the Fen complex, west of the Skien area (Fig. 1) (Andersen, 1987; Andersen and Sundvoll, 1987; Andersen and Taylor, 1988). The "PREMA" source thus appears to have been stationary with respect to southeastern Norway for at least 240 million years prior to the Oslo rifting event. It must consequently have been located in the pre-rift lower lithosphere.

In the Oslo Rift, rocks originating in the HIMU–EM I reservoir have, so far, only been found in the vicinity of the Fen carbonatite complex. It is therefore possible that the HIMU–EM I reservoir formed by mantle metasomatism in connection with the Fen magmatism, and that this reservoir was exhausted during the early phases of partial melting in Permo-Carboniferous time (Anthony et al., 1989). Isotopic contrasts in the mantle at the centimeter-scale between metasomatic veins and a more refractory host lherzolite have been detected in ultramafic xenoliths (H.E.F. Amundsen, pers. commun., 1989). Heating of such a source would first produce melting of the metasomatic veins. As the temperature increased, the veins would become exhausted and melting might progress into the more refractory host.

Implications of mantle reservoirs with respect to rift mechanisms

It was concluded above that two chemically distinct mantle reservoirs have been involved in the Oslo Rift magmatism. One of these reservoirs ("PREMA") was located in the pre-rift lower lithosphere. The location of the other (HIMU–EM I) is unclear, it is possible that it represents a metasomatized part of the pre-rift lithosphere. These results have important consequences with regard to rift mechanisms.

Proposed models for rift initiation may be roughly divided into two categories, passive and active (Sengör and Burke, 1978). In the *passive* models, horizontal stretching causes lithospheric thinning and consequent upwelling of pre-rift

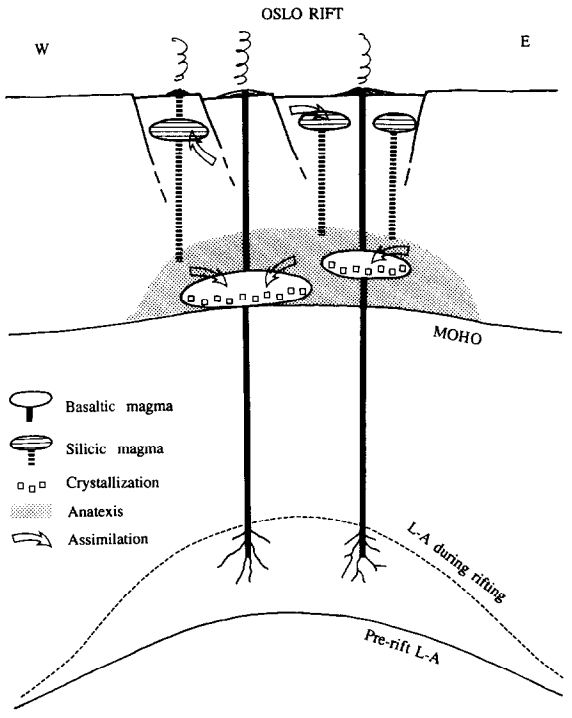

Fig. 11. A schematic model for processes in the crust and upper mantle under the Oslo Rift during the rifting event. $L-A$ = lithosphere–asthenosphere boundary. The figure is not to scale. See text for further discussion.

asthenosphere (e.g., McKenzie, 1978). An important consequence of the passive model is a shift of the isotherms towards lower pressures (a steeper geotherm). Depending on the pre-rift thermal conditions, this might bring parts of the pre-rift lower continental lithosphere above solidus $P-T$ conditions, transforming it into asthenosphere. Magmatism associated with passive rifting should thus primarily sample reservoirs in the pre-rift lower lithosphere. This is indicated schematically in Fig. 11.

In the *active* models, convective upwelling of hot material from deeper levels in the mantle gives rise to partial fusion. Melts originating in the upwelling mantle penetrate into the lithosphere and cause volcanism (e.g., Bott and Kuznir, 1979; Bhattacharji and Koide, 1987). Magmas originating in mantle reservoirs outside the pre-rift lithosphere (referred to below as "foreign" reservoirs) play an important part in active rifting models. However, diapirs of "foreign" melts rising through the lithosphere would represent a thermal pipe

structure in terms of excess heat, which in turn might heat the adjacent lower lithosphere enough to cause partial melting (Neugebauer, 1987). Magmatism associated with active rifting is expected to be dominated by "foreign" melts, but may well include magmas originating in the pre-rift lower lithosphere.

At the present level of information, a passive mechanism is indicated for the Oslo Rift, although an active mechanism cannot be excluded. Information on magmatic products in the southern part of the rift is essential for further progress in this subject.

Implications for the lower crust

It was shown above that the basaltic rocks in Vestfold and Krokskogen were subjected to contamination and crystallization of ol + cpx in the lower crust. Similar results have been obtained in a number of studies on the Oslo Rift (Neumann, 1980, 1988; Neumann et al., 1985, 1988a,b; Rasmussen et al., 1988; Sundvoll et al., 1990). A schematic model for the processes believed to have taken place in the mantle and crust during the rifting event (based on all available data) are given in Fig. 11. Hot magmas ascending from their source in the pre-rift lower lithosphere collected in magma chambers in the lower crust (at depth $\geqslant 15$ km). Crystallization from these magmas produced dense cumulates mainly consisting of olivine and pyroxene. The storage of hot, mafic magmas in the deep crust also led to dehydration, granulite-grade metamorphism and anatexis in the Precambrian country rocks. The anatectic melts caused some contamination of the mantle-derived magmas (as seen in the Vestfold and Krokskogen basaltic lavas), and gave rise to large silicic intrusions in the upper crust. These processes resulted in a transition to denser rock types. The existence of dense cumulates (and residues after partial melting) in the lower crust is confirmed by gravimetric data (Ramberg, 1976; Wessel and Husebye, 1987).

These results imply that processes in the lower crust were important during the Oslo rifting event, and led to permanent changes. It is believed that the processes and changes in different parts of the lithosphere, outlined for the Oslo Rift, are general to intracontinental magmatic events.

Acknowledgements

Thanks are due to T. Enger, H. Hagen and A. Stabel for help with the analytical work. The paper has improved through constructive criticism by B.B. Jensen, W.S. Baldridge and A.K. Pedersen. One of us (E.-R.N.) also wishes to extend special thanks to colleagues in the CREST International Research Team for enlightening discussions on continental rifts and their initiation. The project was financed through a grant from the Norwegian Council for Sciences and Humanities (NAVF). Norwegian ILP Contribution No. 97.

References

Allègre, C.J., Hart, S.R. and Minster, J.-F., 1983. Chemical structure and evolution of the mantle and continents determined by inversion of Nd and Sr isotopic data, II. Numerical experiments and discussion. Earth Planet. Sci. Lett., 37: 191–213.

Andersen, T., 1987. Mantle and crustal components in a carbonatite complex, and the evolution of carbonatite magma: REE and isotopic evidence from the Fen complex, southeast Norway. Chem. Geol., 65: 147–166.

Andersen, T. and Sundvoll, B., 1987. Strontium and neodymium isotopic composition of an early tinguaite (nepheline microsyenite) in the Fen complex, Telemark (southeast Norway): age and petrogenetic implications. Nor. Geol. Unders., 409: 29–34.

Andersen, T. and Taylor, P.N., 1988. Pb isotope chemistry of the Fen carbonatite complex, S.E. Norway: age and petrological implications. Geochim. Cosmochim. Acta, 52: 209–216.

Anthony, E.Y., Segalstad, T.V. and Neumann, E.-R., 1989. An unusual mantle source region for nephelinites from the Oslo Rift, Region, Norway. Geochim. Cosmochim. Acta, 53: 1067–1076.

Bhattacharji, S. and Koide, H., 1987. Theoretical and experimental studies of mantle upwelling, penetrative magmatism, and development of rifts in continental and oceanic crust. Tectonophysics, 143: 13–30.

Bott, M.H.P. and Kuznir, N.J., 1979. Stress distribution associated with compensated plateau uplift structures with application to the continental splitting mechanism. Geophys. J. R. Astron. Soc., 56: 451–459.

Brøgger. W.C., 1933. About rhomb porphyry dykes and accompanying faults in the Oslo Region. Nor. Geol. Unders., 139: 51 pp. (in Norwegian).

Brunfelt, A.O. and Steinnes, E., 1969. Instrumental activation analysis of silicate rocks with epithermal neutrons. Anal. Chim. Acta, 48: 13–24.

Dahlgren, S., 1987. The satelite intrusions in the Fen carbonatite–alkaline rock province, Telemark, southeastern Norway. Cand. Scient. Thesis, University of Oslo, Oslo, 300 pp.

Dons, J.A., 1977. Diabase from Stig, 219 m.y. Nytt Oslofeltgruppen 4, 1972 (printed in 1977): 29–31.

Field, D. and Råheim, A., 1979. Rb–Sr total rock isotope studies on Precambrian charnockitic gneisses from south Norway: evidence for isochron resetting during a low-grade metamorphic–deformational event. Earth. Planet. Sci. Lett., 45: 32–44.

Gordon, G.C., Randle, K., Goles, G.G., Corliss, J.B., Beeson, M.H. and Oxley, S.S., 1968. Instrumental analysis of standard rocks with high-resolution gammaray detectors. Geochim. Cosmochim. Acta, 32: 369–396.

Govindaraju, K., 1984. 1984 compilation of working values for 170 international reference samples of mainly silicate rocks and minerals. Geostandard Newslett., VIII (Spec. Issue).

Hageskov, B. and Pedersen, S., 1981. Rb/Sr whole rock age determinations from the western part of the Østfold basment complex, SE Norway. Bull. Geol. Soc. Den., 29: 119–128.

Hart, S.R., Gerlach, D.C. and White, W.M., 1986. A possible new Sr–Nd–Pb mantle array and consequences for mantle mixing. Geochim. Cosmochim. Acta, 50: 1551–1557.

Henderson, P., 1982. Inorganic Geochemistry. Pergamon Press, Oxford, 353 pp.

Henningsmoen, G., 1978. Sedimentary rocks associated with the Oslo Region lavas. In: J.A. Dons and B.T. Larsen (Editors), The Oslo Paleorift: A Review and Guide to Excursions. Nor. Geol. Unders., 337: 17–24.

Hofmann, A.W., 1988. Chemical differentiation of the Earth: the relationship between mantle, continental crust, and oceanic crust. Earth Planet. Sci. Lett., 90: 297–314.

Hofmann, A.W., Jochum, K.P., Seufert, M. and White, W.M., 1986. Nb and Pb in oceanic basalts: new constraints on mantle evolution. Earth Planet. Sci. Lett., 79: 33–45.

Jacobsen, S.B. and Heier, K.S., 1978. Rb–Sr isotope systematics in metamorphic rocks, Kongsberg sector, south Norway. Lithos, 11: 257–276.

Jacobsen, S.B. and Wasserburg, G.J., 1978. Nd and Sr isotopic study of the Permian Oslo rift. Short Pap., 4th Int. Conf. on Geochronology, Cosmochronology, and Isotope Geology. U.S. Geol. Surv., Open-File Rep., 78-71: 194–196.

Jacobsen, S.B. and Wasserburg, G.J., 1984. Sm–Nd isotopic evolution of chondrites and achondrites, II. Earth Planet. Sci. Lett., 67: 137–150.

Larsen, B.T., 1975. Geology and tectonics of the Oslo rift zone (including tectonic map 1:250,000). Report for the Norwegian Geotecnical Institute, Project No. 74628.

Larsen, B.T. and Sundvoll, B., 1983. The Oslo rift, a high-volcanicity continental rift formed from a Hercynian continent–continent collision. IUGG XVIII General Assembly, Hamburg, Progr. Abstr., 2: 594 (abstract).

Le Bas, M.J., Le Maitre, R.W., Streckeisen, A. and Zanettin, B., 1986. A chemical classification of volcanic rocks based on the total alkali–silica diagram. J. Petrol., 27: 745–750.

McKenzie, D., 1978. Some remarks on the development of sedimentary basins. Earth Planet. Sci. Lett., 40: 25–32.

Mearns, E.W., 1986. Sm–Nd ages for Norwegian garnet peridotite. Lithos, 19: 269–278.

Neugebauer, H.J., 1987. Models of lithospheric thinning. Annu. Rev. Earth Planet. Sci., 15: 421–443.

Neumann, E.-R., 1980. Petrogenesis of the Oslo Region larvikites and associated rocks. J. Petrol., 21: 498–531.

Neumann, E.-R., 1988. Isotopic and petrological relations of the crust and upper mantle under the Oslo Graben, southeast Norway. Norges Geol. Unders., Spec. Publ., 3: 7–13.

Neumann, E.-R., Larsen, B.T. and Sundvoll, B., 1985. Compositional variations among gabbroic intrusions in the Oslo Rift. Lithos, 18: 35–59.

Neumann, E.-R., Andersen, T. and Mearns, E.W., 1988a. Cumulate xenoliths in the Oslo Rift. Contrib. Mineral. Petrol., 98: 184–193.

Neumann, E.-R., Tilton, G.R. and Tuen, E., 1988b. Sr, Nd, and Pb isotope geochemistry of the Oslo rift igneous province, southeast Norway. Geochim. Cosmochim. Acta, 52: 1997–2007.

Neumann, H., 1960. Apparent ages of Norwegian minerals and rocks. Nor. Geol. Tidsskr., 40: 173–191.

Oftedahl, C., 1952. Studies on the igneous rock complex of the Oslo Region, XII. The lavas. Skr. Nor. Vidensk.-Akad. Oslo, I: Mat.-Naturv. Kl. 1952, 3: 64 pp.

Oftedahl, C., 1953. Studies on the igneous rock complex of the Oslo Region, XIII. The cauldrons. Skr. Nor. Vidensk.-Akad. Oslo, I: Mat.-Naturv. Kl. 1953, 3: 108 pp.

Oftedahl, C., 1960. Permian rocks and structures of the Oslo region. In: O. Holtedahl (Editor), Geology of Norway. Nor. Geol. Unders., 208: 298–343.

Olaussen, S., 1981. Marine incursion in Upper Palaeozoic sedimentary rocks of the Oslo Region, southern Norway. Geol. Mag., 118: 281–288.

Øverli, P.E., 1985. A stratigraphic and petrological study of the Horten basalts, B_1-level, southern Oslo Region. Cand. Scient. Thesis, University of Oslo, Oslo, 108 pp. (unpublished; in Norwegian).

Ramberg, I.B., 1976. Gravity interpretation of the Oslo Graben and associated rocks. Nor. Geol. Unders., 337: 194 pp.

Ramberg, I.B. and Larsen, B.T., 1978. Tectonomagmatic evolution, In: J.A. Dons and B.T. Larsen (Editors), The Oslo Paleorift: A Review and Guide to Excursions. Nor. Geol. Unders., 337: 55–73.

Ramberg, I.B. and Morgan, P., 1984. Physical characteristics and evolutionary trends of continental rifts. Proc., 27th Int. Geol. Congr., 7: 165–216.

Rasmussen, E., Neumann, E.-R., Andersen, T., Sundvoll, B., Fjerdingstad, V. and Stabel, A., 1988. Petrogenetic processes associated with intermediate and silicic magmatism in the Oslo Rift, southeast Norway. Mineral. Mag., 52: 293–307.

Sæther, E., 1962. Studies on the igneous rock complex of the

Oslo Region, XVIII. General investigation of the igneous rocks in the area north of Oslo. Skr. Nor. Vidensk.-Akad. Oslo, I: Mat.-Naturv., N. Ser., 1: 184 pp.

Schou-Jensen, E. and Neumann, E.-R., 1988. Volcanic rocks on Jeløya, central Oslo Region: the Mafic lavas. Nor. Geol. Tidsskr., 68: 289–308.

Segalstad, T.V., 1979. Petrology of the Skien basaltic rocks, southwestern Oslo Region, Norway. Lithos, 12: 221–239.

Sengör, A.M.C. and Burke, K., 1978. Relative timing of rifting and volcanism in Earth and its tectonic implications. Geophys. Res. Lett., 5: 419–421.

Skjernaa, L. and Pedersen, S., 1982. The effect of penetrative Scevonorwegian deformations on the Rb–Sr isotope systems in the Rømskog–Aurskog–Høland area, SE Norway. Precamb. Res., 17: 215–243.

Sun, S.-S., 1980. Lead isotopic study of young volcanic rocks from mid-ocean ridges, ocean islands and island arcs. Philos. Trans. R. Soc. London., Ser. A, 297: 409–445.

Sundvoll, B., 1978. Isotope- and trace-element chemistry, geochronology. In: J.A. Dons and B.T. Larsen (Editors), The Oslo Paleorift: A Review and Guide to Excursions. Norg. Geol. Unders., 337: 35–40.

Sundvoll, B. and Larsen, B.T., 1982. Datings of major geological stress indicators in the development of a rift system: the Oslo Paleorift. Terra Cognita, 2: 64.

Sundvoll, B., Neumann, E.-R., Larsen, B.T. and Tuen, E., 1990. Age relations among Oslo Rift magmatic rocks: implications for tectonic and magmatic modelling. In: E.-R. Neumann (Editor), Rift Zones in the Continental Crust of Europe—Geophysical, Geological and Geochemical Evidence: Oslo–Horn Graben. Tectonophysics, 178: 67–87 (this issue).

Taylor, S.R. and McLennan, S.M., 1985. The Continental Crust: Its Composition and Evolution. Blackwell, Oxford, 312 pp.

Tollefsrud, J.I., 1987. A stratigraphic and petrological study of B_1-basalt at Holmestrand, southern Oslo Region. Cand. Scient. Thesis, University of Oslo, Oslo, 133 pp. (unpublished; in Norwegian).

Weaver, B.L. and Tarney, J., 1984. Empirical approach to estimating the composition of the continental crust. Nature, 310: 575–577.

Weigand, P.W., 1975. Studies on the igneous rock complex of the Oslo Region, XXIV. Geochemistry of the Oslo basaltic rocks. Skr. Nor. Vidensk.-Akad. Oslo, I. Mat.-Naturv.., N. Ser., 34: 38 pp.

Wessel, P. and Husebye, E.S., 1987. The Oslo Graben gravity high and taphrogenesis. Tectonophysics, 142: 15–26.

Wood, D.A., 1979. A variably veined suboceanic upper mantle —genetic significance for mid-ocean ridge basalts from geochemical evidence. Geology, 7: 499–503.

Wörner, G., Zindler, A., Staudigel, H. and Schmincke, H.-U., 1986. Sr, Nd, and Pb isotope geochemistry of Tertiary and Quaternary alkaline volcanics from West Germany. Earth Planet. Sci. Lett., 81: 151–162.

Zindler, A. and Hart, H., 1986. Chemical geodynamics. Annu. Rev. Earth Planet. Sci., 14: 493–571.